



# $^{99m}\text{Tc}$ -methoxyisobutylisonitrile single-photon emission computed tomography/computed tomography parathyroid imaging in the diagnosis of functional parathyroid cysts: an initial experience

Yushan Wei<sup>1,2</sup>, Yan Liu<sup>1</sup>, Lulu Yang<sup>1</sup>, Hui Xu<sup>1</sup>, Yiyuan Yang<sup>1</sup>, Yiqian Liang<sup>1</sup>, Yuchen Zhang<sup>1</sup>, Aimin Yang<sup>1</sup>, Xiaojiang Tang<sup>3</sup>, Jianjun Xue<sup>1^</sup>

<sup>1</sup>Department of Nuclear Medicine, the First Affiliated Hospital of Xi'an Jiaotong University, Xi'an, China; <sup>2</sup>Department of Medical Imaging, Xi'an Chest Hospital, Xi'an, China; <sup>3</sup>Department of Breast Surgery, the First Affiliated Hospital of Xi'an Jiaotong University, Xi'an, China

**Contributions:** (I) Conception and design: J Xue; (II) Administrative support: A Yang, J Xue; (III) Provision of study materials or patients: X Tang, Y Yang, Y Wei; (IV) Collection and assembly of data: Y Liu, L Yang, H Xu, Y Yang; (V) Data analysis and interpretation: Y Liu, Y Zhang, J Xue, Y Liang; (VI) Manuscript writing: All authors; (VII) Final approval of manuscript: All authors.

**Correspondence to:** Jianjun Xue, MD, Department of Nuclear Medicine, the First Affiliated Hospital of Xi'an Jiaotong University, 277 West Yanta Road, Xi'an, China. Email: xuejianjun@mail.xjtu.edu.cn.

**Background:** Functional parathyroid cysts (FPCs) are rare and difficult to diagnose with noninvasive methods. The aim of this study was to evaluate the diagnostic value of  $^{99m}\text{Tc}$ -methoxyisobutylisonitrile ( $^{99m}\text{Tc}$ -MIBI) single-photon emission computed tomography/computerized tomography (SPECT/CT) parathyroid imaging in the diagnosis of FPCs and to account for its performance.

**Methods:** The data from 10 patients with suspected parathyroid cysts (PCs) who underwent  $^{99m}\text{Tc}$ -MIBI SPECT/CT parathyroid imaging between 2012 and 2022 were retrospectively evaluated. The diagnostic value of  $^{99m}\text{Tc}$ -MIBI SPECT/CT parathyroid imaging for FPCs was analyzed.

**Results:** Surgical resection was performed in six cases and parathyroid puncture was performed in four cases. The sensitivity of  $^{99m}\text{Tc}$ -MIBI SPECT/CT for FPCs was 100.0% (3/3), with a specificity of 100.0% (7/7) and an accuracy of 100.0% (10/10). The postoperative pathological findings in three cases of FPCs were parathyroid adenoma, parathyroid adenoma with hemorrhage, and parathyroid adenoma with cystic degeneration, respectively. The diagnostic accuracy of ultrasound and CT for PCs was only 22.22% (2/9) and 25.0% (1/4), respectively, and neither modality could indicate whether the cysts were functional or not.

**Conclusions:**  $^{99m}\text{Tc}$ -MIBI parathyroid SPECT/CT imaging has a high value in the diagnosis of FPCs in patients with suspected PCs, and an intense ring-shaped accumulation of radioactivity in the cyst wall on  $^{99m}\text{Tc}$ -MIBI imaging suggests that the patient may have FPCs.

**Keywords:** Parathyroid cyst (PCs); functional parathyroid cysts (FPCs); single-photon emission computed tomography/computed tomography imaging (SPECT/CT imaging);  $^{99m}\text{Tc}$ -methoxyisobutylisonitrile ( $^{99m}\text{Tc}$ -MIBI); hyperparathyroidism (HPT)

Submitted Jun 28, 2023. Accepted for publication Oct 26, 2023. Published online Jan 25, 2024.

doi: 10.21037/gs-23-273

**View this article at:** <https://dx.doi.org/10.21037/gs-23-273>

<sup>^</sup> ORCID: 0000-0002-9188-1362.

## Introduction

Parathyroid cysts (PCs) are relatively rare clinical lesions, which were first described in 1880 via autopsy by Sandström (1) and first reported via surgical treatment in the neck in 1905 by Goris (2). Clinically, PCs can be divided into two categories according to their hormonal activity: functional PCs (FPCs) and non-FPCs (NFPCs). There are about 218 articles in the literature reporting 359 cases of PCs from 1905 to 2016 (3). Common sites for PCs are the anterior neck and mediastinum, and PCs have been reported to account for 1–5% of neck masses (3). In most cases, PCs present with nonspecific symptoms. An asymptomatic mass in the neck is the most common clinical presentation of PC and can sometimes be confused with thyroid nodules, with compressive symptoms being the second most common clinical presentation. NFPCs are often found incidentally, while FPCs may be a rare cause of primary hyperparathyroidism (PHPT), with an estimated prevalence of 2.32% (41/1,769) reported in a large surgical case series by McCoy *et al.* (4). Therefore, the accurate diagnosis of PCs is difficult in clinical practice. The two diseases have been treated differently: patients with NFPCs have generally undergone PC resection and puncture suction or injection of the sclerosing agent after puncture aspiration (5,6), but for those with FPCs, surgical resection

is the only effective treatment.

Ultrasound (US) has been found to be the most useful diagnostic tool for PCs, followed by US-guided fine needle aspiration. US is simple and inexpensive and can detect cystic lesions of the parathyroid gland and differentiate them from solid lesions. It is used as a primary screening tool for PCs in clinical practice and is the modality of choice for guiding fine needle aspiration. Other imaging techniques used to locate PCs include plain radiography, computed tomography (CT), and magnetic resonance imaging (MRI), with surgical exploration being a useful diagnostic tool in some cases.

Hyperparathyroidism (HPT) is a common endocrine disorder resulting from the autonomous overproduction of parathyroid hormone (PTH) by abnormal parathyroid glands (7). The most common causes of PHPT are parathyroid adenomas (~85%), followed by parathyroid hyperplasia (~15%) and parathyroid cancer (<1%) (8), with PC being an extremely rare cause. It is easy to locate a cyst lesion by using examinations of US, CT, or MRI of the neck, but it can be difficult to determine whether the PCs are FPCs or NFPCs.

$^{99m}\text{Tc}$ -methoxyisobutylisonitrile ( $^{99m}\text{Tc}$ -MIBI) can be taken up by mitochondria-rich oxyphil cells in parathyroid lesions, and scintigraphy is based on this principle (9,10); in the case of a single parathyroid adenoma, sensitivity varies from 80% to 100% (11). However, it is often difficult to detect nonfunctioning ectopic parathyroid glands (12). Currently, nuclear  $^{99m}\text{Tc}$ -MIBI imaging is one of the most accurate and reliable means of preoperative parathyroid imaging (13). It plays an important role in HPT not only due to its high sensitivity and detection rate for localizing parathyroid tissue but also due to its ability to aid in assessing the degree of parathyroid hyperplasia before surgery and in selecting partial parathyroid tissue for preservation *in situ* or in autotransplantation during surgery (14). In a meta-analysis of 1,236 cases who underwent  $^{99m}\text{Tc}$ -MIBI single photon emission CT/CT (SPECT/CT) parathyroid imaging before PHPT, the detection rate of  $^{99m}\text{Tc}$ -MIBI SPECT/CT imaging for PHPT was 88% (95% CI: 84–92%) (15).  $^{99m}\text{Tc}$ -MIBI SPECT/CT scintigraphy is the current standard method for detecting hyperfunctioning parathyroid glands (16) and is used as a conventional first-line presurgical imaging method (17), which is typically supplemented by US. PET/CT has recently emerged as a complementary second-line imaging technique with the advantage of a higher resolution and a shorter acquisition time than SPECT/CT (18) while  $^{18}\text{F}$ -fluorocholine ( $^{18}\text{F}$ -FCH) has been proven to

### Highlight box

#### Key findings

- $^{99m}\text{Tc}$ -methoxyisobutylisonitrile ( $^{99m}\text{Tc}$ -MIBI) parathyroid single-photon emission computed tomography/computed tomography imaging has a high value in the diagnosis of functional parathyroid cysts (FPCs) in patients with suspected parathyroid cysts (PCs).

#### What is known and what is new?

- FPCs are rare and difficult to diagnose with noninvasive methods, and the clinical use of  $^{99m}\text{Tc}$ -MIBI imaging for the diagnosis of FPCs is rare, with varying conclusions in case reports.
- $^{99m}\text{Tc}$ -MIBI parathyroid imaging has a high value for the localization of hyperparathyroidism.
- In patients with suspected PCs or elevated cystic fluid parathyroid hormone, an intense ring-shaped accumulation of radioactivity in the cyst wall on  $^{99m}\text{Tc}$ -MIBI imaging suggests that the patient may have FPCs.

#### What is the implication, and what should change now?

- FPCs can be diagnosed clinically using  $^{99m}\text{Tc}$ -MIBI parathyroid imaging.
- Future studies with large samples should be performed to further confirm the value of  $^{99m}\text{Tc}$ -MIBI imaging in FPCs.

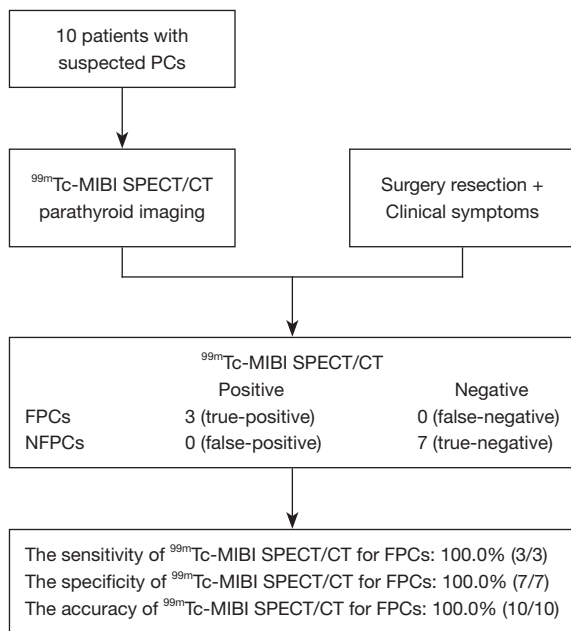


**Figure 1** Study flowchart. PC, parathyroid cyst;  $^{99m}\text{Tc}$ -MIBI,  $^{99m}\text{Tc}$ -methoxyisobutylisonitrile; SPECT, single-photon emission computed tomography; CT, computed tomography; FPC, functional parathyroid cyst; NFPC, non-FPC.

be superior to  $^{99m}\text{Tc}$ -MIBI in previous studies (19–21); however, the disadvantages of PET/CT are that cyclotron-produced radionuclides for PET/CT parathyroid imaging are relatively expensive, and there are no standardized guidelines for image acquisition (16).

Therefore,  $^{99m}\text{Tc}$ -MIBI may be useful in differentiating between FPCs and NFPCs, yet reports of FPCs diagnosed with  $^{99m}\text{Tc}$ -MIBI SPECT/CT are rare. This study was thus conducted to summarize the initial experience of 10 cases of PCs diagnosed with  $^{99m}\text{Tc}$ -MIBI SPECT/CT and with CT and US for comparison. The aim of this study is to highlight the value of  $^{99m}\text{Tc}$ -MIBI SPECT/CT in the diagnosis of FPCs and its possible imaging mechanisms, to improve the understanding of FPC imaging with  $^{99m}\text{Tc}$ -MIBI, and to expand the clinical application of  $^{99m}\text{Tc}$ -MIBI SPECT/CT. We present this article in accordance with the STARD reporting checklist (available at <https://gs.amegroups.com/article/view/10.21037/gs-23-273/rc>).

## Methods

### Research participants

Ten patients, including three males and seven females,

admitted to the First Affiliated Hospital of Xi'an Jiaotong University School of Medicine between 2012 and 2022 for suspected PCs were examined. They had an age range of 20–81 years and a mean age of  $50.0 \pm 16.2$  years. Patient data were analyzed retrospectively (Figure 1). Three cases were admitted with symptoms of HPT; one with abnormal thyroid hormone levels; and the other six cases with incidentally discovered neck masses, which were asymptomatic or with nonspecific symptoms. PC was defined as elevated PTH level in the cystic fluid or parathyroid cells on puncture fluid cytology. FPC was defined as PC with a clinical diagnosis of PHPT or with biochemical changes of PHPT before surgery but excluding vitamin D deficiency, malabsorption, renal disease, and drug-induced factors. In contrast, NPC was defined as PCs with normal serum PTH levels before resection. The clinical diagnosis included FPCs in three cases and NFPCs in seven cases. This study retrospectively analyzed the patients' serum PTH, serum calcium, and serum phosphorus in addition to the results of US, CT, and  $^{99m}\text{Tc}$ -MIBI SPECT/CT parathyroid imaging. The study was conducted in accordance with the Declaration of Helsinki (as revised in 2013). The study was approved by the Institutional Review Board of the First Affiliated Hospital of Xi'an Jiaotong University, Xi'an, China (No. XJTU1AF2021LSL-023), and individual consent was waived for this retrospective analysis.

### $^{99m}\text{Tc}$ -MIBI SPECT/CT

Anterior and posterior planar images of the neck and thorax were acquired with 500 k counts/view 15 min (early phase) and 120 min (delayed phase) after an intravenous injection of 740 MBq (20 mCi) of  $^{99m}\text{Tc}$ -MIBI (Beijing Atom High Tech Co., Ltd., Beijing, China), and a 360° SPECT/CT image was acquired 30 min after intravenous injection. Images were acquired using a Siemens Symbia T16 SPECT/CT scanner (Siemens Healthineers, Erlangen, Germany) equipped with a low-energy, high-resolution collimator (collection energy, 140 KeV; energy window width), a 128×128 matrix, a 360° rotation, a 6° step-and-shoot technique, an acquisition time of 30 s per frame, and a zoom factor of 1.45. The transverse, coronal, and sagittal sections were reconstructed with attenuation correction using Hann filters (cutoff frequency =10) to produce SPECT images.

### Image analysis

The  $^{99m}\text{Tc}$ -MIBI SPECT/CT images were visually

**Table 1** Preoperative laboratory findings and demographic characteristics of 10 patients with PCs

Patient No.	Gender	Age (years)	Serum PTH (15–65 pg/mL)	PTH in cystic fluid (pg/mL)	Serum calcium (2.1–2.51 mmol/L)	Serum phosphate (0.9–1.5 mmol/L)	TH/TSH	TPO-Ab (IU/mL)
1	Female	41	290.8	>5,000	2.64	0.75	N/N	–
2	Male	68	1,714	–	2.83	0.65	–	–
3	Female	81	853	2,050	3.3	0.52	–	–
4	Female	49	46.94	1,395	2.25	1.21	↑/N	>3,000
5	Female	52	51.38	3,080	2.36	1.11	N/N	<15.0
6	Female	41	58.06	1,787	2.22	1.12	N/N	<15.0
7	Male	50	50.38	1,529	2.3	1.03	–	–
8	Male	51	23.7	205.6	2.26	1.36	N/N	–
9	Female	47	74.3	1,152	2.34	1.03	–	–
10	Female	20	47.6	–	2.2	1.13	N/N	–

↑, increase. PC, parathyroid cyst; PTH, parathyroid hormone; TH, thyroid hormone; TSH, thyroid-stimulating hormone; TPO-Ab, thyroid peroxidase antibody; N, normal.

interpreted by two experienced nuclear medicine physicians working independently, and consensus was reached on the findings. Positive  $^{99m}\text{Tc}$ -MIBI SPECT/CT was considered to be a cystic lesion in the parathyroid gland, neck, or mediastinum on CT imaging but no  $^{99m}\text{Tc}$ -MIBI uptake at the cystic lesion site combined with increased  $^{99m}\text{Tc}$ -MIBI uptake in the peripheral margins on SPECT imaging.

### Statistical analysis

The data were analyzed using SPSS version 18.0 (IBM Corp., Armonk, NY, USA). Continuous variables are expressed as the mean  $\pm$  standard deviation and were analyzed with the independent samples *t*-test. Statistical significance was set at  $P < 0.05$ .

## Results

The laboratory and demographic characteristics of the 10 patients are shown in *Table 1*. Preoperatively, all 10 patients had a palpable mass in the neck, and serum thyroid hormone levels and thyroid-stimulating hormone (TSH) tests were performed in 5 cases. All of 10 cases underwent  $^{99m}\text{Tc}$ -MIBI SPECT/CT parathyroid imaging, 9 cases underwent US examination of the neck, and 4 cases underwent CT examination of the neck and upper mediastinum.

### Pathological results

The postoperative pathological findings in three cases of FPCs were parathyroid adenoma, parathyroid adenoma with hemorrhage, and parathyroid adenoma with cystic degeneration, respectively. Three of the seven NFPC cases underwent treatment via operations, two of which were due to recurrence of the cysts after repeated aspiration, with lesion sizes of 28 mm  $\times$  16 mm  $\times$  30 mm and 30 mm  $\times$  25 mm  $\times$  10 mm, respectively; one was due to obvious compression symptoms, with a lesion size of 51 mm  $\times$  39 mm  $\times$  60 mm. In the remaining four cases, no surgery was performed, and parathyroid puncture results were available.

### The results of US, CT, and $^{99m}\text{Tc}$ -MIBI SPECT/CT parathyroid imaging

The diagnostic accuracy of US and CT for cystic lesions was 55.56% (5/9) and 75.00% (3/4), respectively, whereas the accuracy for PCs was only 22.22% (2/9) and 25.0% (1/4), respectively; neither modality could indicate whether the cysts were functional or not. The results of  $^{99m}\text{Tc}$ -MIBI parathyroid SPECT/CT imaging from the 10 patients are shown in *Table 2*. The sensitivity of  $^{99m}\text{Tc}$ -MIBI SPECT/CT for FPCs was 100.0% (3/3), with a specificity of 100.0% (7/7) and an accuracy of 100.0% (10/10). In three cases of FPCs,  $^{99m}\text{Tc}$ -MIBI parathyroid SPECT/CT imaging

**Table 2** Results of US, CT, <sup>99m</sup>Tc-MIBI SPECT/CT parathyroid imaging, pathological findings, and clinical diagnosis in 10 patients with PCs

Patient No.	Lesion size (mm)	<sup>99m</sup> Tc-MIBI SPECT/CT	US	CT	Treatment	Pathology	Clinical diagnosis
1	79×22	Ring-shaped accumulation of radioactivity	Cystic mass in right neck	Tumor of the right thyroid	Surgical excision	Parathyroid adenoma with intracapsular hemorrhage	FPCs
2	46×31	Ring-shaped accumulation of radioactivity	Thyroid adenoma of the left lobe with cystic degeneration	Cyst in the left lobe of the thyroid	Surgical excision	Parathyroid adenomatous hyperplasia with cystic degeneration	FPCs
3	59×37	Ring-shaped accumulation of radioactivity	Lymphatic duct cysts not exclusive of hemangiomas	Parathyroid cyst in the right lobe	Surgical excision	Parathyroid adenoma with cystic degeneration	FPCs
4	28×16×30	Negative	Parathyroid enlargement	Cyst below the left lobe of the thyroid	Surgical excision	PCs	NFPCs
5	51×39×60	Negative	Parathyroid enlargement	–	Surgical excision	PCs (right lobe)	NFPCs
6	34×25	Negative	PCs	–	Nonsurgical	PCs*	NFPCs
7	22×21×31	Negative	Parathyroid enlargement	–	Nonsurgical	PCs*	NFPCs
8	–	Negative	–	–	Nonsurgical	PCs*	NFPCs
9	14×8×20	Negative	Parathyroid enlargement	–	Nonsurgical	PCs*	NFPCs
10	30×25×10	Negative	Left-lower PCs	–	Surgical excision	PCs (left-lower lobe)	NFPCs

\*, the result of US-guided fine needle puncture. US, ultrasound; CT, computed tomography; <sup>99m</sup>Tc-MIBI, <sup>99m</sup>Tc-methoxyisobutylisonitrile; SPECT, single-photon emission CT; PC, parathyroid cyst; FPC, functional PC; NFPC, non-FPC.

showed <sup>99m</sup>Tc-MIBI concentrations in the periphery of the cyst (*Figure 2*), and the postoperative pathological findings were parathyroid adenoma, parathyroid adenoma with hemorrhage, and parathyroid adenoma with cystic degeneration, respectively. In seven cases of NFPCs, no <sup>99m</sup>Tc-MIBI uptake lesions were found in the periphery of the cysts (*Figure 3*); of these seven patients, three underwent surgery, which yielded a pathological diagnosis of PCs, and the remaining four cases underwent parathyroid puncture instead of surgery, with the puncture findings indicating the presence of PCs.

### Follow-up

One of the six surgically resected patients was lost to follow-up; serum PTH, serum calcium, and serum phosphorus levels were normal in five cases at 3 years. In one case, <sup>99m</sup>Tc-MIBI SPECT/CT parathyroid imaging was normal at 6 and 14 months postoperatively, respectively. At postoperative

months 32, 37, and 39, respectively, the serum PTH levels were 26.2, 32.2, and 26.2 pg/mL (15–65 pg/mL); the serum calcium levels were 2.25, 2.21, and 2.13 mmol/L (2.1–2.51 mmol/L); and the serum phosphorus levels were 1.05, 1.06, and 0.92 mmol/L (0.9–1.5 mmol/L). One patient had a cystic fluid PTH level of 1,152 pg/mL and a serum PTH level of 74.3 pg/mL, but a normal serum calcium level led to an initial misdiagnosis of FPCs. However, later follow-up results indicated that serum 25-hydroxyvitamin D, serum PTH, serum calcium, and serum phosphorus levels were normal, and parathyroid US and the US-guided fine needle puncture results indicated PCs. Therefore, the diagnosis was changed to NFPCs.

### Discussion

HPT is divided into PHPT and secondary HPT. Common causes of PHPT include parathyroid adenoma, parathyroid hyperplasia, and parathyroid cancer, but PCs

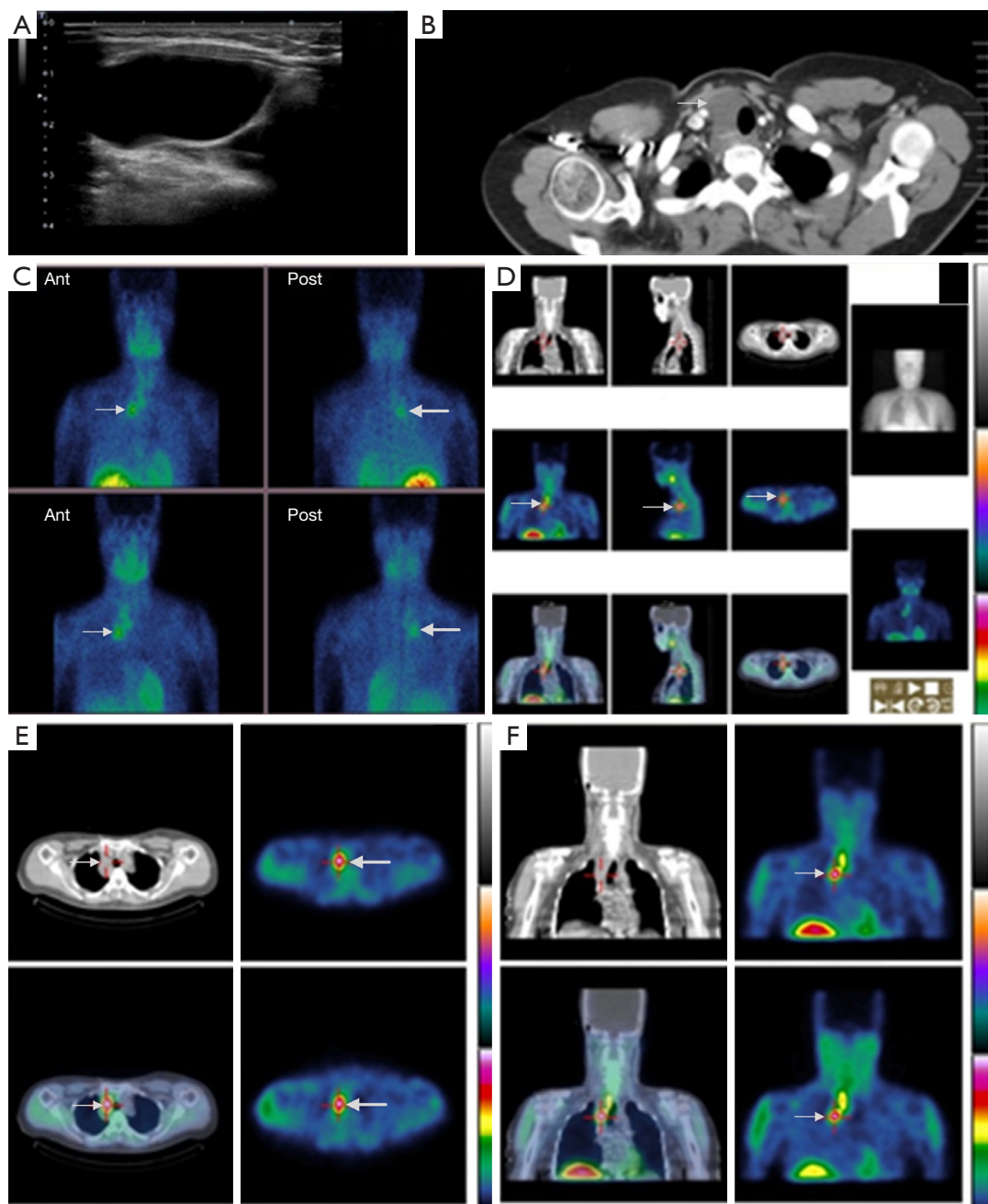


**Figure 2** The positive result of  $^{99m}\text{Tc}$ -MIBI parathyroid imaging for FPCs cases. A 41-year-old woman with a neck mass and elevated PTH levels for 5 months, cyst fluid PTH >5,000 pg/mL, serum PTH 290.8 pg/mL, serum phosphorus 0.75 mmol/L, and serum calcium 2.64 mmol/L. (A) Thyroid B-mode US showed a cystic mass in the right neck. (B) CT enhancement imaging showed a possible tumor (arrow) in the right thyroid gland. (C)  $^{99m}\text{Tc}$ -MIBI parathyroid planar imaging of 20 and 120 min showed focal  $^{99m}\text{Tc}$ -MIBI uptake in the lower right thyroid region (arrows). (D-F) SPECT/CT tomosynthesis imaging showed no obvious radionuclide uptake in the upper part of the lesion, but there was abnormal radionuclide uptake in the lower part of the lesion (arrows), suggesting a lower right HPT with cystic degeneration. Pathology indicated (right) parathyroid adenoma with hemorrhage. Ant, anterior; Post, posterior;  $^{99m}\text{Tc}$ -MIBI,  $^{99m}\text{Tc}$ -methoxyisobutylisonitrile; FPC, functional parathyroid cyst; PTH, parathyroid hormone; US, ultrasound; CT, computed tomography; SPECT, single-photon emission computed tomography; HPT, hyperparathyroidism.

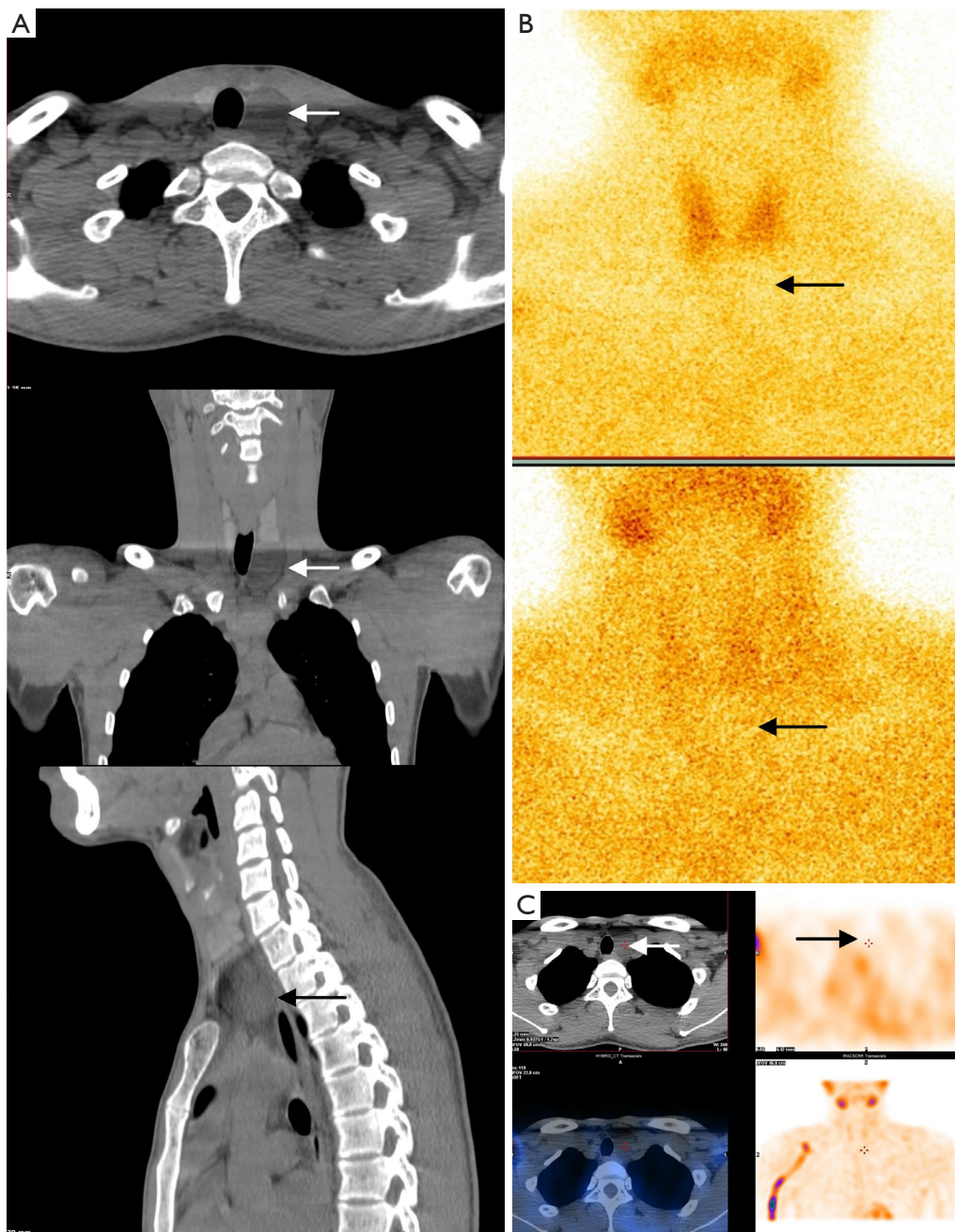


**Figure 3** The negative result of  $^{99m}\text{Tc}$ -MIBI parathyroid imaging for cases with NFPCs. (A) CT imaging. (B) The negative imaging of  $^{99m}\text{Tc}$ -MIBI planar imaging. (C) The negative imaging of parathyroid  $^{99m}\text{Tc}$ -MIBI SPECT/CT. A 47-year-old female patient with normal serum PTH level on examination (47.6 pg/mL). (B,C)  $^{99m}\text{Tc}$ -MIBI planar and SPECT/CT parathyroid imaging showed no significant hyperparathyroid tissue (arrows); postoperative pathological findings showed PCs in the left-lower lobe, and the clinical diagnosis was NFPCs.  $^{99m}\text{Tc}$ -MIBI,  $^{99m}\text{Tc}$ -methoxyisobutylisonitrile; NFPC, non-functional parathyroid cyst; CT, computed tomography; SPECT, single-photon emission computed tomography; PTH, parathyroid hormone; PC, parathyroid cyst.

are an exceedingly rare etiology, with an incidence of only 0.08% to 3.4% among all parathyroid lesions (22). In a retrospective study of 6,621 patients undergoing neck US for various reasons, only 5 PCs were diagnosed, and the overall prevalence of PCs was 0.075% in an unselected population (23). McCoy *et al.* reported an incidence of PCs lesions of 3% (48/1,769) in a large sample of patients treated for PHPT (4).

There are currently around 300 reports of PCs in the literature, with PCs accounting for fewer than 0.01% of all cervical masses (24). Clinically, PCs are classified as NFPCs and FPCs according to serum calcium, serum phosphorus, and serum PTH levels. A network meta-analysis of 218 articles, reporting 359 well-documented cases of PCs, showed that NFPCs were more frequent, representing 61.6% (220/357) of the total number of patients, and had a female predilection (male =26.5%, female =73.5%;  $P<0.0001$ ), whereas FPCs had a slight predominance in the female population (male =48.5%, female =51.5%;  $P<0.001$ ) (3). Clinically, NFPCs and FPCs usually present as a cervical mass, and their preoperative diagnosis is difficult; moreover, FPCs may also manifest with symptoms and signs, such as hypercalcemia and renal or bone damage, that are characteristic of high PTH levels.

The PTH level in the cystic fluid is critical in the diagnosis of PCs. It is generally accepted that during fine needle aspiration biopsy of the cyst, extraction of a thin, clear, and colorless fluid is highly suggestive of PC; if the PTH level is elevated in the cystic fluid or the puncture fluid cytology shows parathyroid cells, the patient also can be diagnosed with PCs (25,26). Regardless of whether the diagnosis is FPCs or NFPCs, PTH in cystic fluid can reach up to two times to thousands of times the normal level, and it has been suggested that the diagnosis of PCs can be established if the PTH level in cystic fluid is higher than its serum level (25) or higher than 1,500 ng/L (27). Albertson *et al.* (28) further summarized the diagnostic criteria for FPCs as follows: (I) the patient has clinical manifestations and biochemical changes of HPT before surgery; (II) the remaining parathyroid gland, except for the cyst, is normal; (III) pathological examination confirms that the cyst wall contains the parathyroid tissue; and (IV) the hyperthyroidism is cured after surgery. However, issues concerning the puncture fluid of PCs remain controversial. It has been argued that the puncture fluid is not conducive to complete surgical resection, as it can increase the chance of recurrence and potentially lead to the implantation of

parathyroid cells in the tissue, resulting in relapse (29).

The pathogenesis of PCs is not completely clear, and a number of theories have been proposed (30-33): (I) PCs develop from the third or fourth branchial cleft remnant during the embryo development process; (II) according to retention theory, increased production or blocked secretion of PTH leads to the emergence of retention cysts; (III) PCs are the residue of the third pharyngeal pouch (Kürsteiner tube) during the embryonic period; (IV) PCs are fused by microcysts within the parathyroid gland or are a large cyst formed by progressive enlargement of a microcyst; (V) PCs are caused by cystic degeneration of the parathyroid adenoma or hemorrhage within the parathyroid adenoma.

The clinical application of  $^{99m}\text{Tc}$ -MIBI imaging for the diagnosis of FPCs is rare, and its results are mixed. Ippolito *et al.* (34) considered that PCs had no function and that FPCs were caused by cystic degeneration of the parathyroid adenoma or PCs combining with parathyroid adenoma. Makino *et al.* reported that  $^{99m}\text{Tc}$ -MIBI was only taken up by the cyst wall of FPCs, suggesting that the mass originated from the parathyroid gland (35), and their study included an intense ring-shaped accumulation of radioactivity in the cyst wall on  $^{99m}\text{Tc}$ -MIBI imaging in three cases of FPC, further confirming this view.

In our study, a 41-year-old female (*Figure 2*) had a neck mass and elevated PTH levels for 5 months, cystic fluid PTH >5,000 pg/mL, serum PTH 290.8 pg/mL, serum phosphorus 0.75 mmol/L, and serum calcium 2.64 mmol/L. Thyroid US suggested a cystic mass in the right neck. In chest CT, there was a low-density shadow in the lower part of the right thyroid lobe, which stretched downward into the right superior mediastinum. Regarding CT enhancement, the right thyroid showed a long striped cystic low-density lesion, with a size of about 79 mm × 22 mm, and the CT value was about 39 Hounsfield units (HU); a patchy shadow with slightly higher density could be observed in the lower margin of the lesion, the CT value was about 149 HU, and disordered, small-blood-vessel shadows were observed. The lower margin of the lesion was involved downward to the area at level of the bronchial bifurcation behind the superior vena cava in the mediastinum, and the lesion was closely associated with the trachea and adjacent blood vessels, suggesting a possible tumor in the right thyroid.  $^{99m}\text{Tc}$ -MIBI parathyroid planar imaging and SPECT/CT tomosynthesis imaging showed an intense ring-shaped accumulation of radioactivity in the cyst wall (*Figure 2*). A translucent cyst was intraoperatively



observed in the posterior lower part of the right thyroid lobe and extended along the right wall of the trachea toward the right superior mediastinum, and it was lobulated and had spacers. The cystic fluid was clear, the cystic wall was thin and did not adhere to the surrounding tissue, and the parathyroid adenoma tissue was visible underneath the cystic wall. Pathology (Figure 2, right panel) indicated parathyroid adenoma with hemorrhage.

Ippolito *et al.* (34) suggested that NFPCs are nonfunctional, whereas FPCs are pseudocysts, essentially caused by cystic degeneration or hemorrhage and necrosis of the parathyroid adenoma. Since NFPCs may be caused by the fusion of microcysts or the fusion of embryonal remnants,  $^{99m}\text{Tc}$ -MIBI imaging does not show nuclear uptake in the diagnosis of NFPCs. Ippolito *et al.*'s perspective may account for the  $^{99m}\text{Tc}$ -MIBI imaging being negative in NFPCs and positive in FPCs. Our study also confirms the above view that  $^{99m}\text{Tc}$ -MIBI imaging is useful for the diagnosis of FPCs but has difficulties in diagnosing NFPCs. Meanwhile, the uptake of  $^{99m}\text{Tc}$ -MIBI is mainly related to the solid portion after cystic degeneration of parathyroid adenoma. When the solid portion is small, microscopic pathological changes may be similar to those of PCs and manifest as a thin-walled cyst with a single lumen. Therefore, it has been suggested (34) that the FPCs reported in the literature might have arisen due to the cystic degeneration of parathyroid adenoma.

Among the typical causes of HPT, parathyroid adenoma and hyperplasia are common and easily distinguished clinically from PCs. Parathyroid carcinoma is also highly rare and characterized by extremely high serum PTH and serum calcium levels; most parathyroid carcinomas are functional, and the symptoms are related to the severity of hypercalcemia. US and CT are quite effective in distinguishing a solid lesion from a cystic lesion (36) and can differentiate PCs from parathyroid carcinoma. Rare cases of cystic parathyroid carcinoma have been reported (37-39), and the differential diagnosis between PCs and cystic parathyroid adenocarcinoma is highly challenging because both essentially have similar preoperative clinical presentations and laboratory results, such as typical symptoms of PHPT, elevated serum PTH and calcium levels, and very high concentrations of PTH in the cystic fluid. US and CT can also make it difficult to determine whether PCs are FPCs or NFPCs. In this study, three cases of FPCs were diagnosed and localized with  $^{99m}\text{Tc}$ -MIBI SPECT/CT imaging, whereas, US and CT respectively

diagnosed these cases as neck cystic mass; thyroid adenoma with cystic degeneration; and lymphatic duct cyst and thyroid tumor, thyroid cyst, and parathyroid cystic degeneration. The sensitivity of  $^{99m}\text{Tc}$ -MIBI SPECT/CT for FPCs reported by McCoy *et al.* (4) was 68% (25/37), but in this study, it was 100.0%, which may be related to the small number of cases examined. The sensitivity of SPECT/CT for FPCs is higher than that of CT and US. This indicates that  $^{99m}\text{Tc}$ -MIBI has high sensitivity and specificity for the diagnosis or localization of FPCs, with advantages that cannot be matched by US and CT. Therefore,  $^{99m}\text{Tc}$ -MIBI parathyroid imaging may be the preferred noninvasive diagnostic or localization method when FPCs are suspected in clinical practice. Although  $^{99m}\text{Tc}$ -MIBI SPECT/CT parathyroid imaging demonstrates good performance for the localization of FPCs, potential drawbacks must be considered before adopting this modality for the diagnosis or localization of FPCs. According to current guidelines (16), preoperative imaging is not recommended for diagnostic purposes but only for the localization of abnormal parathyroid glands in patients with HPT. In this study, seven patients with elevated serum PTH and normal serum calcium levels underwent  $^{99m}\text{Tc}$  SPECT/CT for various reasons, and it is debatable whether it was necessary.

In contrast, seven cases with NFPCs had negative  $^{99m}\text{Tc}$ -MIBI SPECT/CT imaging, suggesting that  $^{99m}\text{Tc}$ -MIBI imaging has no value in the diagnosis of NFPCs. In this study, one patient with NFPCs who was initially misdiagnosed with normocalcemic PHPT had a significantly elevated cystic fluid PTH level (1,152 pg/mL), mildly elevated PTH levels in three tests, and consistently normal calcium levels, and thus vitamin D deficiency, malabsorption, and renal disease-related and some drug-related secondary HPT conditions were excluded. In the follow-up of this patient, normocalcemic PHPT was suspected, and it was suggested that drugs affecting PTH levels such as bisphosphonates, anticonvulsants, diuretics, lithium, denosumab, and phosphorus be excluded in the follow-up. Subsequently, in a more recent follow-up study, this patient's serum 25-hydroxyvitamin D, PTH, calcium, and phosphorus levels were reported to be normal, and the results of parathyroid US and US-guided fine needle puncture showed PCs. Therefore, the diagnosis of this patient was changed from normocalcemic PHPT to NFPCs. The definition of normocalcemic PHPT is the persistently elevated serum PTH levels in the presence of consistently normal albumin-corrected and ionized calcium levels after

exclusion of other causes of PTH elevation (40), and it is most widely accepted as being an early form of classic PHPT (40). According to the European Expert Consensus Statement, normocalcemic PHPT can be considered when there is a persistent biochemical signature (>3 months) of elevated PTH levels in a setting of consistently normal total, albumin-adjusted, and/or free ionized calcium levels according to serial laboratory measurements and when all secondary causes of PTH elevation have been excluded (41). Cusano *et al.* followed up with 108 patients provisionally identified as normocalcemic PHPT for 8 years: only 1.6% (1/64) were confirmed, and 20% (13/64) went on to show evidence of normocalcemic PHPT (42). Normocalcemic PHPT is an exclusionary diagnosis that can only be considered after careful evaluation of the causes of secondary HPT and should be made with great caution.

False-negative  $^{99m}\text{Tc}$ -MIBI parathyroid scans in FPCs did not occur in this study possibly due to the small number of cases, but these have been reported previously. Ak and Acikalin (43) reported a case of confirmed 30 mm × 42 mm × 35 mm FPCs by pathological findings, and Yalcin *et al.* (44) reported a case of 24 mm × 19 mm × 16 mm FPCs without  $^{99m}\text{Tc}$ -MIBI uptake. The most likely reason for this is that  $^{99m}\text{Tc}$ -MIBI uptake is mainly related to a low abundance of parathyroid cells remaining after the cystic degeneration of the parathyroid adenoma. If the solid part is small, the microscopic pathological changes may be similar to those in PCs and may manifest as a thin-walled cyst with a single lumen. The mass contains a large amount of cystic fluid and lacks blood supply, which may be another reason for false-negative  $^{99m}\text{Tc}$ -MIBI images. Additionally, the reasons for false-negative results of  $^{99m}\text{Tc}$ -MIBI imaging may be related to the following factors (45,46): (I) the parathyroid lesions are too small; (II) the cells express excessive P-glycoprotein, resulting in increased  $^{99m}\text{Tc}$ -MIBI transport in cells that accelerates elution; and (III) the proportions of chief cells and acidophilic cells contained in the parathyroid adenoma are too low, or the mitochondrial density in the PCs cells is low.

Several limitations to this study should be noted. First, in terms of design, we employed a single-center, retrospective, nonrandomized design due to ethical and guideline restrictions. Second, the sample size in this study was relatively small due to the low incidence of PCs, which is a significant limitation, and thus the generalizability of our findings may be limited. Therefore, given these limitations, a large-sample, long-term study should be performed in

the future to further confirm the value of MIBI imaging in FPCs.

If the results of SPECT/CT parathyroid scintigraphy are negative, equivocal, or inconsistent with US findings, or if HPT persists or recurs after surgery, alternative evaluation with the hybrid PET/CT technique is recommended (18). There is an increasing amount of evidence suggesting that PET/CT has high sensitivity in localizing hyperfunctioning parathyroid glands. In the study of Mathey *et al.*, 18F-FCH showed a significantly higher sensitivity and accuracy compared with  $^{11}\text{C}$ -methionine and could diagnose a higher number of cases; it was thus considered the preferred modality for localizing of PHPT lesions (17). Recently published parathyroid imaging guidelines suggest that 18F-FCH PET/CT is a potential alternative first-line option in patients with PHPT when its implementation is possible (16) and may be helpful for future applications of PET/CT in the diagnosis or localization of NFPCs.

## Conclusions

PCs can be accurately diagnosed via histological examination or elevated PTH levels in the cystic fluid. According to current guidelines and clinical practice, the role of SPECT/CT parathyroid scintigraphy is to localize hyperfunctional parathyroid lesions. In our study, parathyroid imaging with  $^{99m}\text{Tc}$ -MIBI was proven to be highly valuable in the diagnosis or localization of FPCs. In patients with PHPT or elevated cystic fluid PTH levels, parathyroid imaging with  $^{99m}\text{Tc}$ -MIBI showing no uptake of  $^{99m}\text{Tc}$ -MIBI in the cystic lesion site combined with increased uptake of  $^{99m}\text{Tc}$ -MIBI in the peripheral margins suggests that the patient may have FPCs.

## Acknowledgments

The scientific guarantor of this publication is Dr. Jianjun Xue from Department of Nuclear Medicine, the First Affiliated Hospital of Xi'an Jiaotong University, Xi'an, China.

*Funding:* This study was supported by the Clinical Research of the First Affiliated Hospital of Xi'an Jiaotong University, Xi'an, China (No. XJTU1AF2021CRF-024).

## Footnote

*Reporting Checklist:* The authors have completed the STARD

reporting checklist. Available at <https://gs.amegroups.com/article/view/10.21037/gS-23-273/rc>

*Data Sharing Statement:* Available at <https://gs.amegroups.com/article/view/10.21037/gS-23-273/dss>

*Peer Review File:* Available at <https://gs.amegroups.com/article/view/10.21037/gS-23-273/prf>

*Conflicts of Interest:* All authors have completed the ICMJE uniform disclosure form (available at <https://gs.amegroups.com/article/view/10.21037/gS-23-273/coif>). The authors have no conflicts of interest to declare.

*Ethical Statement:* The authors are accountable for all aspects of the work in ensuring that questions related to the accuracy or integrity of any part of the work are appropriately investigated and resolved. The study was conducted in accordance with the Declaration of Helsinki (as revised in 2013). The study was approved by the Institutional Review Board of the First Affiliated Hospital of Xi'an Jiaotong University, Xi'an, China (No. XJTU1AF2021LSL-023), and individual consent was waived for this retrospective analysis.

*Open Access Statement:* This is an Open Access article distributed in accordance with the Creative Commons Attribution-NonCommercial-NoDerivs 4.0 International License (CC BY-NC-ND 4.0), which permits the non-commercial replication and distribution of the article with the strict proviso that no changes or edits are made and the original work is properly cited (including links to both the formal publication through the relevant DOI and the license). See: <https://creativecommons.org/licenses/by-nc-nd/4.0/>.

## References

- Sandström IV. On a new gland in man and several mammals – glandulae parathyroideae. *Upsala Läk Förenings Förh* 1879–1880;15:441-71.
- Goris D. Extirpation of three cystic parathyroid lobules. *Ann Soc Belge Chir* 1905;5:394.
- Papavramidis TS, Chorti A, Pliakos I, et al. Parathyroid cysts: A review of 359 patients reported in the international literature. *Medicine (Baltimore)* 2018;97:e11399.
- McCoy KL, Yim JH, Zuckerbraun BS, et al. Cystic parathyroid lesions: functional and nonfunctional parathyroid cysts. *Arch Surg* 2009;144:52-6; discussion 56.
- Diaz A, Chavez J, Hemmrich M, et al. Large non-functioning substernal parathyroid cyst: A case report and review of the literature. *Int J Surg Case Rep* 2022;93:106989.
- Sung JY, Baek JH, Kim KS, et al. Symptomatic nonfunctioning parathyroid cysts: role of simple aspiration and ethanol ablation. *Eur J Radiol* 2013;82:316-20.
- Wilhelm SM, Wang TS, Ruan DT, et al. The American Association of Endocrine Surgeons Guidelines for Definitive Management of Primary Hyperparathyroidism. *JAMA Surg* 2016;151:959-68.
- Krishnaraju VS, Saikia UN, Bhadada SK, et al. Cystic Parathyroid Adenomas: An Enigmatic Entity and Role of Tc-99 m Sestamibi Scintigraphy. *Endocr Pract* 2021;27:614-20.
- Carpentier A, Jeannotte S, Verreault J, et al. Preoperative localization of parathyroid lesions in hyperparathyroidism: relationship between technetium-99m-MIBI uptake and oxyphil cell content. *J Nucl Med* 1998;39:1441-4.
- Kunstman JW, Kirsch JD, Mahajan A, et al. Clinical review: Parathyroid localization and implications for clinical management. *J Clin Endocrinol Metab* 2013;98:902-12.
- Pogosian K, Karonova T, Ryzhkova D, et al. (11)C-methionine PET/CT and conventional imaging techniques in the diagnosis of primary hyperparathyroidism. *Quant Imaging Med Surg* 2023;13:2352-63.
- Mahoney EJ, Monchik JM, Donatini G, et al. Life-threatening hypercalcemia from a hepatocellular carcinoma secreting intact parathyroid hormone: localization by sestamibi single-photon emission computed tomographic imaging. *Endocr Pract* 2006;12:302-6.
- Mohamed HE, Bhatia P, Aslam R, et al. Robotic transaxillary and retroauricular parathyroid surgery. *Gland Surg* 2015;4:420-8.
- Ma J, Yang J, Chen C, et al. Use of (99m)Tc-sestamibi SPECT/CT imaging in predicting the degree of pathological hyperplasia of the parathyroid gland: semi-quantitative analysis. *Quant Imaging Med Surg* 2021;11:4375-88.
- Treglia G, Sadeghi R, Schalin-Jäntti C, et al. Detection rate of (99m) Tc-MIBI single photon emission computed tomography (SPECT)/CT in preoperative planning for patients with primary hyperparathyroidism: A meta-analysis. *Head Neck*. 2016;38 Suppl 1:E2159-72.

16. Petranović Ovcariček P, Giovanella L, Carrió Gasset I, et al. The EANM practice guidelines for parathyroid imaging. *Eur J Nucl Med Mol Imaging* 2021;48:2801-22.
17. Mathey C, Keyzer C, Blocklet D, et al. (18)F-Fluorocholine PET/CT Is More Sensitive Than (11)C-Methionine PET/CT for the Localization of Hyperfunctioning Parathyroid Tissue in Primary Hyperparathyroidism. *J Nucl Med* 2022;63:785-91.
18. Imperiale A, Taïeb D, Hindié E. (18)F-Fluorocholine PET/CT as a second line nuclear imaging technique before surgery for primary hyperparathyroidism. *Eur J Nucl Med Mol Imaging* 2018;45:654-7.
19. Graves CE, Hope TA, Kim J, et al. Superior sensitivity of (18)F-fluorocholine: PET localization in primary hyperparathyroidism. *Surgery* 2022;171:47-54.
20. Mazurek A, Dziuk M, Witkowska-Patena E, et al. The utility of 18F-fluorocholine PET/CT in the imaging of parathyroid adenomas. *Endokrynol Pol* 2022;73:43-8.
21. Morris MA, Saboury B, Ahlman M, et al. Parathyroid Imaging: Past, Present, and Future. *Front Endocrinol (Lausanne)* 2021;12:760419.
22. Silva R, Cavadas D, Vicente C, et al. Parathyroid cyst: differential diagnosis. *BMJ Case Rep* 2020;13:e232017.
23. Cappelli C, Rotondi M, Pirola I, et al. Prevalence of parathyroid cysts by neck ultrasound scan in unselected patients. *J Endocrinol Invest* 2009;32:357-9.
24. McKay GD, Ng TH, Morgan GJ, et al. Giant functioning parathyroid cyst presenting as a retrosternal goitre. *ANZ J Surg* 2007;77:297-304.
25. Pontikides N, Karras S, Kaprara A, et al. Diagnostic and therapeutic review of cystic parathyroid lesions. *Hormones (Athens)* 2012;11:410-8.
26. Rossi ED, Revelli L, Giustozzi E, et al. Large non-functioning parathyroid cysts: our institutional experience of a rare entity and a possible pitfall in thyroid cytology. *Cytopathology* 2015;26:114-21.
27. Silverman JF, Khazanie PG, Norris HT, et al. Parathyroid hormone (PTH) assay of parathyroid cysts examined by fine-needle aspiration biopsy. *Am J Clin Pathol* 1986;86:776-80.
28. Albertson DA, Marshall RB, Jarman WT. Hypercalcemic crisis secondary to a functioning parathyroid cyst. *Am J Surg* 1981;141:175-7.
29. Rattner DW, Marrone GC, Kasdon E, et al. Recurrent hyperparathyroidism due to implantation of parathyroid tissue. *Am J Surg* 1985;149:745-8.
30. Jha BC, Nagarkar NM, Kochhar S, et al. Parathyroid cyst: a rare cause of an anterior neck mass. *J Laryngol Otol* 1999;113:73-5.
31. Takashima S, Nakano H, Minamoto K, et al. A thoracoscopically resected case of mediastinal parathyroid cyst. *Acta Med Okayama* 2005;59:165-70.
32. Cao H, Lai CK, Head CS, et al. Cystic parathyroid presenting as an apparent thyroid goiter. *Eur Arch Otorhinolaryngol* 2008;265:1285-8.
33. Armstrong J, Leteurtre E, Proye C. Intraparathyroid cyst: a tumour of branchial origin and a possible pitfall for targeted parathyroid surgery. *ANZ J Surg* 2003;73:1048-51.
34. Ippolito G, Palazzo FF, Sebag F, et al. A single-institution 25-year review of true parathyroid cysts. *Langenbecks Arch Surg* 2006;391:13-8.
35. Makino T, Sugimoto T, Kaji H, et al. Functional giant parathyroid cyst with high concentration of CA19-9 in cystic fluid. *Endocr J* 2003;50:215-9.
36. Ujiki MB, Nayar R, Sturgeon C, et al. Parathyroid cyst: often mistaken for a thyroid cyst. *World J Surg* 2007;31:60-4.
37. El-Housseini Y, Hübner M, Boubaker A, et al. Unusual presentations of functional parathyroid cysts: a case series and review of the literature. *J Med Case Rep* 2017;11:333.
38. Vazquez FJ, Aparicio LS, Gallo CG, et al. Parathyroid carcinoma presenting as a giant mediastinal retrotracheal functioning cyst. *Singapore Med J* 2007;48:e304-7.
39. Tsoli M, Angelousi A, Rontogianni D, et al. Atypical manifestation of parathyroid carcinoma with late-onset distant metastases. *Endocrinol Diabetes Metab Case Rep* 2017;2017:17-0106.
40. Schini M, Jacques RM, Oakes E, et al. Normocalcemic Hyperparathyroidism: Study of its Prevalence and Natural History. *J Clin Endocrinol Metab* 2020;105:e1171-86.
41. Bollerslev J, Rejnmark L, Zahn A, et al. European Expert Consensus on Practical Management of Specific Aspects of Parathyroid Disorders in Adults and in Pregnancy: Recommendations of the ESE Educational Program of Parathyroid Disorders. *Eur J Endocrinol* 2022;186:R33-63.
42. Cusano NE, Maalouf NM, Wang PY, et al. Normocalcemic hyperparathyroidism and hypoparathyroidism in two community-based nonreferral populations. *J Clin Endocrinol Metab* 2013;98:2734-41.
43. Ak I, Acikalin MF. Hyperparathyroidism with a functioning parathyroid cyst. *Clin Nucl Med* 2007;32:713-5.
44. Yalcin Y, Mete T, Aktimur R, et al. A case of primary hyperparathyroidism due to intrathyroidal parathyroid cyst. *J Assoc Physicians India* 2015;35:308-10.

45. Bleier BS, LiVolsi VA, Chalian AA, et al. Technetium Tc 99m sestamibi sensitivity in oxyphil cell-dominant parathyroid adenomas. *Arch Otolaryngol Head Neck Surg* 2006;132:779-82.
46. Xue J, Liu Y, Yang D, et al. Dual-phase 99mTc-MIBI imaging and the expressions of P-gp, GST- $\pi$ , and MRP1 in hyperparathyroidism. *Nucl Med Commun* 2017;38:868-74.

(English Language Editor: J. Gray)

**Cite this article as:** Wei Y, Liu Y, Yang L, Xu H, Yang Y, Liang Y, Zhang Y, Yang A, Tang X, Xue J. <sup>99m</sup>Tc-methoxyisobutylisonitrile single-photon emission computed tomography/computed tomography parathyroid imaging in the diagnosis of functional parathyroid cysts: an initial experience. *Gland Surg* 2024;13(1):32-44. doi: 10.21037/gs-23-273